



HAL
open science

On the usability of event zero time determinations using radioxenon isotopic activity ratios given the real atmospheric background observations

Kassoum Yamba, Martin B. Kalinowski, Oumar Sanogo

► To cite this version:

Kassoum Yamba, Martin B. Kalinowski, Oumar Sanogo. On the usability of event zero time determinations using radioxenon isotopic activity ratios given the real atmospheric background observations. *Journal of Environmental Radioactivity*, 2019, 208, pp.106014 -. 10.1016/j.jenvrad.2019.106014 . hal-03487371

HAL Id: hal-03487371

<https://hal.science/hal-03487371>

Submitted on 20 Dec 2021

HAL is a multi-disciplinary open access archive for the deposit and dissemination of scientific research documents, whether they are published or not. The documents may come from teaching and research institutions in France or abroad, or from public or private research centers.

L'archive ouverte pluridisciplinaire **HAL**, est destinée au dépôt et à la diffusion de documents scientifiques de niveau recherche, publiés ou non, émanant des établissements d'enseignement et de recherche français ou étrangers, des laboratoires publics ou privés.



Distributed under a Creative Commons Attribution - NonCommercial 4.0 International License

On the usability of event zero time determinations using radioxenon isotopic activity ratios given the real atmospheric background observations

Authors

Kassoum YAMBA¹, Martin B. KALINOWSKI², Oumar SANOGO¹,

¹Centre National de la Recherche Scientifique et Technologique (DE/IRSAT/CNRST),
Ouagadougou, Burkina Faso

²Comprehensive Nuclear Test-Ban Treaty Organization (IDC/CTBTO), Vienna, Austria

Corresponding author

Kassoum YAMBA

Centre National de la Recherche Scientifique et Technologique (IRSAT/CNRST)
Institut de Recherche en Sciences Appliquées et Technologiques (IRSAT)
Département Energie (DE)
DE/IRSAT/CNRST
03 BP 7027 Ouagadougou – Burkina Faso
Phone: +22670032683
E-mail : yamba.kassoum@yahoo.com
_fairlir@yahoo.fr

1

2 Keywords

3 Dating, Isotopic activity ratio, Radioxenon, CTBT, Nuclear explosion, Radionuclide event
4 characterization,

5

6 Highlights

- 7 1. Radioxenon data from nuclear reactor releases and medical isotopes production
8 facilities were characterized.
- 9 2. Three typical statistical values were evaluated and took as reference points of release
10 from NPPs and MIPFs.
- 11 3. The zero time using CTBT-relevant radioxenon data set from nuclear tests and nuclear
12 reactor releases were evaluated.
- 13 4. The age precision differences were determined using the calculated ages associated to
14 the real ages of release.

15

16 Abstract

17 This work focuses on the usability of event zero time determination using xenon isotopic
18 activity ratios. Two data sets from Nevada underground nuclear test and Fukushima accident
19 debris were used to calculate the age of radioxenon release by considering three kinds of
20 radioactivity release radionuclide sources: nuclear explosion scenarios, nuclear power reactor
21 release and medical isotopes production facilities release. Typical nuclear power reactor
22 releases were characterized and reference values are proposed for six isotopic activity ratios,
23 which data can be considered as reference point of nuclear reactor effluents at the time of
24 their release obtained from real observations. The same reference values of isotopic activity
25 ratio are given for medical isotopes production facilities releases. The purpose of this study is
26 to evaluate the use of zero-time calculation for source characterization under the assumption
27 that a hypothesis about the event time is made. The event time information may come from a
28 seismo-acoustic event of interest or an inverse atmospheric transport simulation or other
29 context information. For both data sets used in this study, the age precisions are calculated
30 and the time precision difference is evaluated and used as a parameter for the characterization
31 of each radionuclide event. Almost all radioxenon isotopic activity ratios are found to
32 correctly identifying the source type of the radionuclide events studied in this work. The
33 results from this radionuclide events characterization study may be helpful for event screening
34 activities of the Comprehensive Nuclear Test Ban Treaty Organization (CTBTO).

35 1. Introduction

36 The Comprehensive Nuclear-Test-Ban Treaty (CTBT) is an international legal instrument
37 banning any nuclear tests anywhere on the earth (underground, on-ground, in water, and
38 atmosphere). Some radioisotopes of xenon namely Xe-135, Xe-133m, Xe-133 and Xe-131m
39 are considered as most relevant indicators in nuclear explosion monitoring (DE GEER L.-E.
40 et al., 2001) because they are fission products with high probability of being released and
41 detected. The observation of these radioisotopes may be indicative of a nuclear explosion and

42 observations meeting certain screening criteria like an abnormal concentration are considered
43 a radionuclide event for the purpose of nuclear explosion monitoring. Plots of activity ratios
44 for one pair of isotopes vs. another pair of isotopes in logarithmic scale can be used to
45 characterize the source of the emission and most importantly to discriminate between nuclear
46 reactors and nuclear explosions (Kalinowski and Pistner, 2006). By considering the nuclei
47 ratio or isotopic activity ratio of measured radionuclides, it is possible to evaluate their time of
48 release (age of release) (Nir-El, 2004, 2006).

49 It has also been shown that the age determination using isotopic activity ratios is very
50 sensitive to some decay parameters like decay constants (Yamba et al., 2016b). In that work,
51 decay data used come from nuclear databases such as the French NUCLEIDE from
52 Laboratoire National Henry Becquerel (LNHB - CEA) (LNHB, 2017), the US Evaluated
53 Nuclear Data structure File (ENSDF) from National Nuclear Data Center (NNDC, 2017). The
54 nuclear database NUCLEIDE has updated some CTBT-relevant radioxenon decay data
55 Within the framework of the DDEP (Decay Data Evaluation Project) project (Galan, 2017;
56 Galan et al., 2018).

57 When IMS facilities of CTBTO detect a CTBT-relevant radionuclide it is crucial to determine
58 its source characteristics including the time origin of the fission reaction and of the release of
59 the observed radionuclides. The activities of different isotopes reported in IMS measurements
60 are usable for event time calculation. In theory, event dating works well under the assumption
61 of a nuclear explosion scenario (Yamba et al., 2018b). For the radioxenon isotopes, the
62 operational challenge is to understand results of event dating applied to the normal
63 background noise. The routine IMS atmospheric background observations result from normal
64 operational releases of nuclear facilities.

65 The goal of this study is to estimate the usefulness of the timing equations in light of the real
66 observations. It aims at characterizing conditions under which reasonable origin times can be
67 determined and under which discrimination between nuclear test signatures and normal
68 atmospheric background could work.

69 Two data sets were used for this study: (a) Local observations of radioxenon after nuclear
70 tests at the Nevada Test Site; (b) Observations of reactor sources with a known radioxenon
71 source term, i.e. IMS observations with strong contribution of the Fukushima accident
72 (Yamba et al., 2016a, 2017a, 2017b, 2018a).

73 Let us note that the results of measurements made in radio-xenon monitoring facilities of the
74 Comprehensive Nuclear Test Ban Treaty Organization (CTBTO) are available both as
75 activities at acquisition start and converted into activity concentrations at collection stop. The
76 activities are used in this work for evaluating the release age of radionuclide events (Axelsson
77 and Ringbom, 2014; Yamba et al., 2015).

78 While age determination from isotopic ratios is not new, the innovation of this paper is to
79 investigate whether age determinations under certain source type assumptions applied to
80 routine observations with atmospheric background from various sources can be used to
81 discriminate possible sources and even identify the source type to be a nuclear test or a
82 nuclear reactor release simply based on a comparison between the age determined from
83 isotopic ratios and the age of an assumed source type.

84

2. Xenon isotopic activity ratio at zero time

One of the most important information in the activity ratio formula that is used to calculate the time of a radionuclide event is the initial isotopic activity ratio (activity ratio at zero time or at the time of release). That initial activity ratio is easily understandable in the nuclear explosion case, by using independent and cumulative fission yields (according to the situation) of the isotope of interest. Values of these fission yields can be found in a nuclear data bank like ENSDF (Evaluated Nuclear Structure Data File).

The initial activity ratios that is to be considered for Nuclear Power Plants (NPPs) release and Medical Isotopes Production Facilities (MIPFs) are not fixed values. In considering a nuclear reactor running in steady state during a long time, the equilibrium level can be calculated for each activity ratio of interest. Measurements made and reported by operators of Nuclear Power Plants on the gaseous effluents are the basis of a statistical study of radioxenon releases from NPPs (Kalinowski and Tuma, 2009). These data are used to determine the distribution of radioxenon isotopic ratios resulting from the batch mode with a median value, an upper and a lower limit. The same approach was taken with regard to the CTBT-relevant radioxenon isotopes that are determined by Kalinowski/Grosch/Hebel (2014) to be typically released from medical isotopes production facilities. These values are very important in characterizing the source time of a radionuclide-monitoring event because they are based on the real observations. Figure 1 shows the distribution of the xenon isotopic activity ratios measured at the stack of nuclear power plants and expected at medical isotopes production facilities.

Figure 1: Distribution of radioxenon activity ratios using nuclear reactor (NPP) release data (Kalinowski and Tuma, 2009) and medical isotopes production facility (MIPF) release estimates (Kalinowski/Grosch/Hebel, 2014). Only batch release mode was considered for the nuclear event characterization in this study.

Table 1 summarizes the three statistical parameters of the logarithmic distribution namely median value, upper limit and lower limit (both excluding outliers) for NPPs using best estimates based on real observations for the six xenon activity ratios: Xe-135/Xe-133m, Xe-135/Xe-133, Xe-135/Xe-131m, Xe-133m/Xe-133, Xe-133m/Xe-131m and Xe-133/Xe-131m. These values can be compared with those used for the isotopic ratio screening flags that are implemented as indicator of a radionuclide event of potential interest radionuclide event in the radionuclide analysis reports issued by the International Data Center (IDC) of CTBTO. The current screening levels in radionuclide event discrimination at IDC/CTBTO are explained by (Postelt, 2014). Three threshold values are currently used for the activity ratio Xe-133m/Xe-131m it is 2, for Xe-135/Xe-133 it is 5 and for Xe-133m/Xe-133 it is 0.3. According to table 1, the upper limits that can be expected for these activity ratios to be released from NPPs are 6.3, 0.14 and 0.023 when using the whisker limits of Figure 1 and disregarding the outliers. As a result, NPP releases may cause the screening flag for Xe-133m/Xe-131m to indicate a potential event of interest to nuclear explosion monitoring but not for the other two isotopic ratio screening flags.

128 *Table 1: Reported xenon activity ratios from nuclear reactors releases, measured by Nuclear*
129 *Power Plants (NPP) in United States and Europe during 2006, 2009 and 2014. Only the*
130 *batch release cases were considered.*

131

132 Table 2 presents the lower limit, median and upper limit values of radioxenon isotopic activity
133 ratios from medical isotopes production facilities (MIPFs) releases. The considered batch
134 releases of radioxenon are from European Union and United States (Gueibe et al., 2017). The
135 upper limits that can be expected from MIPFs for the activity ratios used for screening flags
136 are 53 (Xe-133m/Xe-131m), 2.3 (Xe-135/Xe-133) and 0.043 (Xe-133m/Xe-133). As a result,
137 like for NPPs also MIPF releases may cause only the screening flag for Xe-133m/Xe-131m to
138 indicate a potential event of interest. However, MIPFs are much more likely than NPPs to
139 raise this flag.

140 The radioxenon activity data values provided in Table 1&2 are very important in radionuclide
141 event characterization, especially in radionuclide event zero time determination. These
142 isotopic activities values combined with cumulative and independent fission yields allow for
143 describing together the change over time of the radioxenon isotopic activity ratios of interest
144 for the CTBTO-relevant radionuclide event, namely the nuclear explosion scenarios (under
145 in-growth condition and full fractionation). These need to be distinguished from the range of
146 isotopic activity ratios that can be observed as background resulting from the range of nuclear
147 reactor releases as characterized by NPPs upper limit, NPPs lower limit and NPPs median
148 value, and to be distinguished as well from the possible medical isotope production facilities
149 release scenarios (MIPFs upper limit, MIPFs lower limit and MIPFs median value).

150 *Table 2: Reported xenon activity ratios from medical isotopes production facility (MIPF)*
151 *releases. Only the batch release cases were considered.*

152

153

154 3. Relevant xenon activity as a function of time

155 Some radioxenon isotopes such as ^{135}Xe , $^{133\text{m}}\text{Xe}$, ^{133}Xe and $^{131\text{m}}\text{Xe}$ are considered as relevant
156 for CTBT nuclear explosion monitoring. Remote detections of an underground nuclear test
157 are most likely associated with a sudden release (a prompt or delayed but short-term release)
158 of fission products (Kalinowski, 2011). We can consider two extreme kinds of sudden release
159 of radioactivity: release of gaseous fission products following a full fractionation from their
160 precursors and radioactivity release in a composition that developed under in-growth
161 condition. In the first case, xenon gas escapes immediately after the end of fission reactions;
162 and in the second case, xenon gas stay mixed with its precursors until being released.

163 The comprehensive analytical formulas giving the numbers of nuclides $N_{\text{Xe}135}(t)$, $N_{\text{Xe}133}(t)$,
164 $N_{\text{Xe}133\text{m}}(t)$, $N_{\text{Xe}131\text{m}}(t)$ used in this work can be found in (Yamba et al., 2018b).

165 Figure 2 shows the change over time of isotopic activity ratios of CTBT-relevant radioxenons
166 as they develop over time as calculated using the analytical equations of the radioxenons
167 decay process for two nuclear explosion scenarios (under in-growth condition and full
168 fractionation). For comparison, the three nuclear reactor release levels (using NPPs upper

169 limit, NPPs lower limit and NPPs median value) and three levels of medical isotopes
170 production facilities (using MIPFs upper limit, MIPFs lower limit and MIPFs mean value) are
171 plotted as well in two ways. One way is a straight line and representing a fresh release that
172 might occur at any time after the time zero of the nuclear explosion scenarios. The second
173 way is also starting at time zero but following the radioactive decay with time progressing to
174 represent a release from a nuclear facility that coincides with the nuclear explosion scenarios.
175 Figure 2 is an update of similar plots published in (Kalinowski et al., 2010).

176

177

178 *Figure 2: Change over time of isotopic activity ratios of CTBT-relevant radionuclides for two*
179 *kinds of release from a nuclear explosion, and three indicative values of release from NPP*
180 *and MIPF releases (minimum, median and maximum). The latter are shown as constants as*
181 *well in order to account for the fact that such fresh pulse releases can occur at any time after*
182 *the assumed time zero of a nuclear explosion scenario.*

183 One important conclusion from Figure 2 is that for the first hours or days the isotopic ratios of
184 nuclear explosion scenarios are higher than even the highest NPP and MIPF release ratios.
185 Sooner or later, the activity ratios of nuclear explosion scenarios lose their uniqueness due to
186 the radioactive decay moving the ratio below the level that can occur with fresh releases from
187 nuclear facilities. However, as long as the isotopic ratios are in a domain that can only be
188 reached by nuclear explosion scenarios, the attempt of calculating an event time will not be
189 possible for the assumptions of NPP or MIPF releases. Once the isotopic activity ratios have
190 reached a level that can occur from nuclear tests as well as nuclear facilities, the event time
191 that is derived from an observed isotopic activity will be earlier (i.e. older and longer delay
192 before being observed) for the fully fractionated nuclear explosion scenario and later (i.e.
193 younger) under the assumption of a release from a nuclear facility. The in-growth version of a
194 nuclear explosion scenario is cutting through the nuclear facility release curves and the
195 determined ages may either be earlier or later radionuclide event.

196 A more robust discrimination of nuclear explosions against civilian sources, particularly
197 releases from nuclear reactors is possible by using two different isotopic activity ratios,
198 because this discrimination method proposed by (Kalinowski et al., 2010) is independent on
199 the time elapsed between generation detection. It is also independent of a delay between
200 generation and the release into the atmosphere. Figure 3 shows how the trajectories of two
201 different activity ratios plotted against each other are changing with time progressing, namely
202 Xe^{135}/Xe^{133} against Xe^{133m}/Xe^{131m} . The nuclear explosion under in-growth condition is
203 very close to the release from medical isotopes production facilities for which maximum,
204 minimum and mean values are found in a very narrow band along the decay path.

205

206 *Figure 3: Change of radionuclide activities ratios Xe^{135}/Xe^{133} against Xe^{133m}/Xe^{131m}*
207 *according to the kind of releases. The initial isotopic activity ratios (activity ratios at the*
208 *release) used for nuclear reactor releases (NPP-median, NPP-limitLOW and NPP-limitUP)*
209 *and medical isotopes production facilities releases (MIPF-mean, MIPF-min and MIPF-max)*
210 *are respectively from Table1 and Table2. The square red dots represent debris released from*
211 *Fukushima accident as observed at IMS stations.*

212

213 4. Age determination using real observations data

214 4.1. Using Nevada data

215 A detailed atmospheric radioactivity release information for 433 nuclear tests conducted on
216 the Nevada Test Site from 15 September 1961 through 23 September 1992 has been analysed
217 in (Kalinowski et al., 2014, 2010; Kalinowski and Pistner, 2006; Kalinowski and Tuma, 2009)
218 and (Schoengold et al., 1996). The importance of the use of Nevada underground nuclear test
219 data in radionuclide event characterization is that they come from real observations following
220 nuclear explosions on the Nevada site where the atmospheric releases are considered to be
221 from prompt venting or from operational release. It is also demonstrated that atmospheric
222 signature of an underground nuclear test could result from a late-time surface flux which is
223 too diffuse to be detected off-site (Carrigan et al., 2019). Schoengold et al. (1996) is not
224 describing the measurement procedure in detail. Therefore, it is not clear whether all
225 radioxenon isotopes are real observations. In some cases, a lead radionuclide or a gross
226 activity may have been measured and the activity release of other isotopes may have been
227 calculated using an evolution model. Figure 4 shows the distribution of xenon isotopic
228 activity ratios calculated using these reported data from the US underground nuclear
229 explosions. As we can see in, the isotope Xe-131m is almost absent in the reported data so
230 that the isotopic activity ratios including the isotope Xe-131m are almost missing.

231

232 *Figure 4: Distribution of the valid activity ratios using Nevada nuclear explosion data. We*
233 *can notice that the ratios including Xe-131m, namely Xe-135/Xe-131m, Xe-133/Xe-131m and*
234 *Xe-133m/Xe-131m are almost absent.*

235

236 In this paper, we are evaluating the use of zero-time calculation for source characterization
237 under the assumption that a hypothesis about the event time is made. The event time
238 information may come from a seismo-acoustic event of interest or an inverse atmospheric
239 transport simulation or other context information. In this scenario, any observed radioxenon
240 signals with two or more isotopes would be evaluated by comparing the known age
241 (difference between observation date and zero-time) with the one calculated from isotopic
242 ratios under different source-type assumptions: nuclear explosion (fully fractionated or with
243 in-growth), NPPs and MIPFs taking the full range of the latter two into consideration.

244 In order to evaluate which source hypothesis gives the best match, the age precision is defined
245 as the calculated age divided by the known age of the release. With this definition, the true
246 radioactivity release scenario will have an age precision closest to 1. The physical meaning of
247 the term “age precision” is to be a measure for source time agreement with the value 1
248 implying perfect agreement or in other words the age discrepancy with this being the worse
249 the higher above 1 the value of age precision is. Figures 5 show the distribution of age
250 precision calculated using data from Nevada underground nuclear explosions. As we can see
251 in Figure 5, a nuclear explosion case (in black colour) gives the closest age precision to 1,
252 unlike the NPPs and MIPFs release cases where the age precisions are relatively far from 1. In
253 most cases, the nuclear test with in-growth is the best match but in a few instances, the full
254 fractionation scenario yields the better age precision, confirming the findings of (Kalinowski,
255 2011). The NPP scenario is almost never getting an age precision close to 1 whereas some

256 extreme MIPF signatures provide a good match with an age precision close to 1 and can be
257 confused with a nuclear explosion signal. It should be noted that this study assumes the
258 special condition that the origin time of all release scenarios is the same and constrained from
259 context information like a seismic event. Whereas this is realistic for a nuclear explosion,
260 emissions from nuclear facilities could take place at any time. The constrained made here
261 applies for the case of having the release time constraint, e.g. from results of atmospheric
262 transport modelling. Further studies will deal with the more general case of allowing for any
263 release time from nuclear facilities and more general with possible mixing of radioactivity
264 from multiple sources.

265

266

267 *Figure 5: Distribution of the evaluated age precision according to the kind of release. Useful*
268 *Nevada xenon activity ratios were used in the time algorithms for Nuclear explosions (full*
269 *fractionation and under in-growth conditions), NPPs release (median, lower limit and upper*
270 *limit values), MIPFs release (mean, min and and max values). The ideal age precision shown*
271 *in magenta colour is normalized to 1.*

272 The fact that the nuclear explosions scenario has the best precision and, therefore, appears as
273 the most probable explanation of a radioxenon observation confirms the expectation (these
274 observations are all known to be releases from underground nuclear test explosions) and it
275 provides an evidence for the discrimination capability of the age estimate.

276

277 4.2. Using Fukushima debris data

278 Fukushima nuclear accident occurred in Japan took place over several days following the
279 Great East Japan Earthquake off the Pacific coast of Japan on 11 May 2011. The earthquake
280 generated a huge tsunami and its waves overwhelmed the tsunami barriers of the Fukushima
281 Daiichi nuclear power plant (NPP) site. They flooded the primary and backup power systems
282 and equipment, as well as the ultimate heat sink systems and structures, of all six units on the
283 site. Following the off-site power loss that occurred before the tsunami due to the earthquake
284 damage to the transmission system, the flooding caused also the loss of on-site power sources
285 and on-site power distribution systems. Units 1–5 of the Fukushima Daiichi NPP experienced
286 extended station blackout (SBO) events, which exceeded nine days in Units 1 and 2, and 14
287 days in Units 3 and 4.

288 The nuclear units were unable to cope with the extended loss of electrical power. As a
289 consequence, there was no sufficient plant heat removal and the reactors of Units 1, 2 and 3
290 suffered damage as the fuel overheated and melted. The reactor pressure vessels (RPVs) that
291 enclose the reactor cores were eventually crashed in those units, and radioactive material
292 escaped from the reactors. The radioactive material confined in the primary containment
293 vessels (PCVs) was further released directly to the environment either in a controlled manner,
294 i.e. by venting of the reactors' PCVs, or in an uncontrolled manner upon damage and failure
295 of the confinement structures (INTERNATIONAL ATOMIC ENERGY AGENCY, 2015).

296 The important dates of reference from that accident for our work are the following, where the
297 time is given in UTC:

298

- 299 • At 15:36 on 12 March 2011, an explosion occurred on the service floor of the Unit 1
300 RB (reactor building), causing extensive damage to the upper building structure.
- 301 • At 11:01 on 14 March, an explosion occurred in the upper part of the Unit 3 RB
302 (reactor building), destroying the building structure above the service floor.
- 303 • At 06:14 on 15 March, an explosion was heard on the site, and tremors were felt in the
304 common MCR (main control room) of Units 1 and 2. The available information
305 indicated a possible PCV (primary containment vessel) failure and the possibility of
306 uncontrolled releases from Unit 2 (INTERNATIONAL ATOMIC ENERGY
307 AGENCY, 2015).

308 Thus in light of that accident description above reported by International Atomic Energy
309 Agency, we can consider as the first time of release on 12 March 2011, 15:30. That release
310 was the largest in total activity. It lasted for several hours but had the highest release rate at its
311 beginning. Using this start time as reference for the age determination is a simplification but
312 sufficient for the purpose of this study. Figure 6 shows the distribution of xenon isotopic
313 activity ratios calculated using reported xenon data from IMS (Fukushima debris data), where
314 the NPPs limits and the median value from Fukushima accident are displayed. Except the
315 ratio Xe135/Xe133, all median values from Fukushima accident are included in the range of
316 NPPs release.

317 In general, only the very early observations have both isotopes detected above the MDC.
318 Their isotopic activity ratios are consistent with the median and the box-and-whisker
319 distributions of the Fukushima releases. However for most isotope pairs, the observations are
320 quite different. They are scattering around the ratio of the longer-lived of the two isotopes
321 with respect to the detection limit of the shorter-lived isotope. With time progressing, they are
322 following the trend of the radioactive decay of the longer-lived isotope until eventually, the
323 ratio converges towards unity when both isotope's concentrations are close or below the
324 detection limit.

325

326 *Figure 6: Distribution of the activity ratios using Fukushima accident debris data. Data used*
327 *in this study were recorded from 14/03/2011 to 31/05/2011 in many IMS radionuclide*
328 *stations. Black colour is used for valid entries for which both isotopes are above MDC, i.e.*
329 *real detections that can be quantified; a bright grey is used in case one of the two isotopes is*
330 *above MDC (in general it is the longer lived one of both); a dark grey indicates ratios that*
331 *are calculated with both isotopes below MDC and basically scatter around the ratio of both*
332 *isotopes detection limit, i.e. close to 0 in the logarithmic scale (indicated by a green line).*

333 In the Figure 6, the fitting curves are obtained by using the exponential function (like decay
334 curve) expressed as $y=a.exp(b.x)$ where a and b are constants generated when the fitting curve
335 tool (of MATLAB in our case) is used. By writing FP =[a;b] a fitting parameter, its value is
336 found to be $FP(Xe135/Xe133) = [28.3;-1.0890]$, $FP(Xe135/Xe133m) = [55.4;-0.8944]$,
337 $FP(Xe135/Xe131m) = [32.69;-0.8574]$, $FP(Xe133m/Xe131m) = [1.8650;-0.1748]$,
338 $FP(Xe133/Xe131m) = [77.32;-0.05284]$, $FP(Xe133m/Xe133) = [1.6000;-0.1441]$. Let us
339 notice that these fitting parameters are obtained by using the early observations within a few
340 days after the fresh releases of the Fukushima accident. This timeframe is selected to make
341 sure that both isotopes are real observations and the activity ratio is valid. As we can see in
342 Figure 6, the fitting curves in magenta color closely consistent with activity ratios decay
343 curves. The distribution of xenon isotopic ratios in Figure 6 is such that the later observations
344 are not consistent with the decay curves that are decreasing over time. For the three upper

345 plots with Xe-135, the later observations follow an upward trend. This can be explained by
346 Xe-135 being either false positives close to detection limit or replaced by the MDC value. The
347 slope is therefore indicating the decay of the longer lived isotopes until they also reach their
348 respective MDC and the isotopic ratio approaches the MDC ratio which is marked by the
349 green horizontal line.

350
351 Any radioxenon observation with two or more isotopes would be evaluated by comparing the
352 known age (difference between observation date and zero-time) with one calculated from
353 isotopic ratios under different source-type assumptions: nuclear explosion (fully fractionated
354 or with in-growth), NPPs and MIPFs taking the full range of the latter two into consideration.
355 As for the Nevada nuclear test data, we are evaluating the use of zero-time calculation for
356 source characterization of IMS observations following the Fukushima accident under the
357 assumption that a hypothesis about the event time is made. The ages of releases calculated
358 using xenon isotopic activity ratios are divided by the age with to 12 March 2011, 15:30 as
359 the assumed date of the release to get the age precision. Figure 7 show the distribution of age
360 precision calculated using data from Fukushima accident debris, where - except for the ratio
361 of Xe-133/Xe-133m - the NPPs release case gives the closest age precision to 1, unlike the
362 nuclear explosion scenarios or MIPFs release cases which have the age precisions relatively
363 far from 1. It is remarkable that determining the ages of Fukushima debris provides the best
364 precision for the range of NPP releases (between minimum and maximum) without making
365 use of the knowledge of the estimated isotopic activity ratios that were released from the
366 Fukushima Daiichi NPPs. With time progressing, the quality of the age precision deteriorates.
367 This is due to the concentrations getting closer to normal atmospheric background and the
368 detection limits. Sooner or later, the age determination seems to be in high precision for
369 different of nuclear source types. With different delays after the Fukushima accident, four out
370 of the six isotopic activity ratios achieve a high time precision for the nuclear explosion
371 scenario. This implies that the activity ratios observed on Fukushima debris for four pairs of
372 isotopes could have been miss-interpreted as signals appearing like those of a nuclear
373 explosion. However, the isotopic ratios apparently matching the signature of a nuclear test
374 appear at different delays after the original release and result in inconsistent zero-times for the
375 hypothesis of a nuclear explosion origin. Therefore, the activity ratios of different pairs of
376 radioxenon isotopes observed after Fukushima debris can be used to prove that nuclear
377 explosions can be excluded as the possible source of these detections.

378

379

380 *Figure 7: Distribution of the evaluated age precision according to the kind of release. Useful*
381 *activity ratios from Fukushima accident debris were used in the time algorithms for Nuclear*
382 *explosions (full fractionation and under in-growth conditions), NPPs release (median, lower*
383 *limit and upper limit values), MIPFs release (mean, min and and max values). The ideal age*
384 *precision shown in magenta colour is normalized to 1.*

385

386 5. Possible discrimination approach using event timing

387 When radioxenon facilities for the International Monitoring System (IMS) record an
388 radionuclide event involving radioxenon, e.g. at an abnormal concentration, it is important to

389 get information that can be used to characterize and identify the source and most importantly
390 whether that observation may come from a possible nuclear test explosion. It might result
391 from an accident but most frequently, it is caused from a normal operational release of a
392 nuclear power plant (NPPs) or from a medical isotope production facility (MIPF).

393 One possible approach of event characterization is to investigate how radionuclide event age
394 determination can contribute to the identification of the source of a radioactivity release. In
395 this study, we work under the limiting assumption that a hypothesis for the source time is
396 available from context information like a seismo-acoustic event of interest or from
397 atmospheric transport simulations. For this purpose, two data sets were used and evaluated
398 ages were proposed according to the kind of radioactivity release: a nuclear explosion and a
399 nuclear reactor accident release, both characterized by a sudden release. The first data set
400 (reported data from Nevada underground nuclear explosions) is studied with reported times of
401 origin for each xenon isotope recorded. The second case of Fukushima debris data is used
402 with the assumption that a known first part of the release is dominating. This assumption is
403 justified by the fact that the first batch release of radionuclides from Fukushima accident that
404 started on 12 Mars 2011, around 15:00 (INTERNATIONAL ATOMIC ENERGY AGENCY,
405 2015) contained a large part of the cumulative release from all Fukushima Daiichi reactors.

406 The ages of radioactivity releases calculated using xenon isotopic activity ratios are used with
407 known dates of release to evaluate the age precision assuming three kinds of radioactivity
408 sources: nuclear explosion, NPPs and MIPFs. The time precision difference is defined as the
409 difference between the perfect time precision value and the found time precision. Thus, a
410 radionuclide event having the lowest values of time precision difference is considered as the
411 most probable, because giving the best time precision. This approach consisting of using the
412 time precision difference could be useful for identifying a radionuclide event.

413 Table 3 presents the results from the statistical analysis of the age precision differences
414 obtained using activities data from Nevada nuclear test site. The median values are considered
415 for each radionuclide event of interest. Except for the activity ratio Xe_{133}/Xe_{131m} , it appears
416 that the nuclear explosion under in-growth condition is the most probable event, because the
417 time precision difference values for that event are the lowest. Except for Xe_{133}/Xe_{131m} , this
418 approach of using the time precision difference as a screening parameter in radionuclide event
419 characterization is successfully validated because it identifies correctly nuclear explosions to
420 be the source of all radionuclide events of all radioxenon activities in the data set used in
421 Table 3 that are known to originate from underground nuclear explosions at the Nevada test
422 site. Since this paper is a proof-of-concept, the uncertainties of historic data are not reflected
423 and the age precision difference is presented with more significant digits than can be justified
424 by the uncertainties of the test data set. Four significant digits are simply used for illustrative
425 purposes to be able to rank the results and avoid any two values to be the same due to
426 rounding effects.

427

428 *Table 3: Evaluation of the time precision difference obtained by making the difference*
429 *between the perfect time precision value and the found time precision. The observation data*
430 *used are from Nevada underground nuclear test. Plutonium Pu-239 and Uranium U-235 are*
431 *used as the nuclear explosion materials fission induced by fission energy neutrons.*

432

433

434 Table 4 present the results from the statistical analysis of the age precision differences
435 obtained using activities data from Fukushima accident debris. The median values are
436 considered for each radionuclide event of interest. Except for the activity ratio
437 Xe^{133}/Xe^{133m} , it appears that the nuclear reactor release scenario is the most probable event,
438 because the time precision difference values for that event are the lowest. Effectively, the
439 radioxenon activities data used in Table 4 are consistent with operational releases from
440 Nuclear Power Plants (Fukushima Daiichi), i.e. these observations can be characterized as
441 originating from a NPP without making use of the known activity ratios that are known to
442 have been released from the Fukushima accident.

443 *Table 4 : Evaluation of the time precision difference obtained by making the difference*
444 *between the perfect time precision value and the found time precision. The observation data*
445 *used are from Fukushima accident debris. Plutonium Pu-239 and Uranium U-235 are used as*
446 *the nuclear explosion materials fission induced by fission energy neutrons.*

447

448 The results of the time precision difference given in Tables 3&4 are obtained by using as
449 fission material in the two nuclear explosion scenarios uranium-235 and plutonium-239 with
450 the fission neutron energy. Except for one ratio in each case, the results from the time
451 precision difference analysis are in accordance with the nature of the radionuclide events.
452 From Table 3, 4 out of the 5 available activity ratios yield good results allowing identifying
453 the radionuclide event (80%). By using Table 4, we can see that 5 out of all 6 activity ratios
454 (more than 80%) show good results of time precision differences that have allowed
455 identifying as NPPs release as the source of the radionuclide event. So we can notice that
456 almost all radioxenon isotopic activity ratios are correctly identifying the source type of the
457 studied radionuclide events.

458 The quality of the source hypothesis test based on age determination can be assessed by
459 calculating the statistics for true positives and false negatives for the two variants of the
460 nuclear test hypothesis as well as false positives and true negatives for NPPs and MIPFs
461 release if radioxenon isotopic activities from real nuclear test are used (data from Nevada test
462 in this study). The same approach is apply for calculating the statistics for true positives and
463 false negatives for the whole range of NPPs release hypothesis (ages from minimum to
464 maximum isotopic activity ratios) while true negative and false positive are calculated for
465 nuclear tests and MIPFs hypothesis. A confusion matrix has been used and the results are
466 given in the Tables 5&6 where the four parameters True Positive (TP), False Positive (FP),
467 True Negative (TN) and False Negative (FN) are presented.

468 *Table 5: Statistics obtained using a confusion matrix. Activities data used are from Nevada*
469 *test. For each nuclear event, five (05) isotopic activity ratios are considered.*

470

471 The statistics True Positive and False Negative are evaluated for the nuclear explosion under
472 in-growth condition while the statistics True Negative and False Positive are evaluated for the
473 cases of nuclear explosion with full fractionation, NPP release and MIPF release. The true

474 class is defined as ‘*nuclear explosion*’ and the false class ‘*non-nuclear explosion*’. The reality
475 is that all activity data used are from underground nuclear explosions. The statistics from
476 Table 5 indicate that the scenario ‘*nuclear explosion under in growth condition*’ is the most
477 accurate.

478

479 *Table 6: Statistics obtained using a confusion matrix. Activities data used are from*
480 *Fukushima accident. For each nuclear event, six (06) isotopic activity ratios are considered.*

481

482 The statistics True Positive and False Negative are evaluated for NPP release scenario while
483 the statistics True Negative and False Positive are evaluated for the cases of nuclear explosion
484 with full fractionation, nuclear explosion under in-growth condition and MIPF release. The
485 true class is defined as ‘*NPP release*’ and the false class ‘*non-NPP release*’. The reality is that
486 all activity data used are from NPP release (Fukushima accident). The statistics from Table 6
487 indicate that the scenario ‘*NPP release*’ is the most accurate.

488

489 6. Discussion & conclusion

490 This work focused on the usability of event zero time determinations using xenon isotopic
491 activity ratios given the real atmospheric background observations. Two data sets from real
492 observations were used to calculate the age precisions of radionuclide release: radionuclide
493 activity data from Nevada test site and radionuclide concentration data from Fukushima
494 accident debris. For the purpose of this investigation, three kinds of radionuclide events are
495 distinguished: the nuclear explosions scenarios (full fractionation and under in-growth
496 conditions), the nuclear power plants (NPPs) releases (NPP-median, NPP-lower limit and
497 NPP-upper limit values), the medical isotopes production facilities (MIPFs) releases (MIPFs -
498 mean, MIPFs -min and MIPFs -max values).

499 The radionuclide event screening parameter proposed in this work is the age precision
500 differences. This parameter is interpreted such that the most probable radionuclide event is the
501 one that has the lowest value.

502 The first data set is from Nevada nuclear test site where United States performed underground
503 nuclear explosions from 15/09/1961 to 23/09/1992. The interpretation of the age precision
504 difference shows that a nuclear explosion under in-growth condition assumption is found to
505 be the most likely source of the observed radionuclide events. This can be considered a
506 validation of this screening approach since it confirms the known kind of the radionuclide
507 event.

508 The second data set is from Fukushima nuclear accident in May 2011 in Japan, where the
509 radioactivity release started by the explosion of the reactor 1 on 12 March 2011, at 15:30.
510 From our study, it is found that the nuclear power plant release gives the most accurate results
511 because the age precision difference values are the lowest for that type of event. Again, this
512 can be considered another validation of this screening approach since that is the correct kind
513 of source of the radioactivity releases.

514 In summary, the radionuclide event age determination using radioxenon isotopic activity ratio
515 is usable for characterizing a radionuclide event, by evaluating the age precision difference as
516 an event screening parameter. The radionuclide event with the lowest value of this screening
517 parameter can be identified as the type of source that is to the origin of the radioxenon release
518 into the environment. However, let us note that the age precision evaluation is validated only
519 for the cases with a known suspected date. It is also shown that the activity ratio Xe-133/Xe-
520 131m is not reliable for discriminating between nuclear explosions and nuclear facilities using
521 this new approach of radionuclide event characterization because its age precision results are
522 less exacts. The age discrimination using the Xe133/Xe133m ratio cannot distinguish well a
523 NPP source from a MIPF source but avoids misinterpretation of an NPP source as originating
524 from a nuclear test.

525 This work can be improved by taking into account more parameters related to radioactivity
526 release characterization such as possible delay of release from the underground. That will
527 need to consider more kind of nuclear explosion releases. This issue could be one of future
528 investigations. It may also be useful to investigate results of the event origin time calculation
529 for the case of no hypothesis available about the time of the release.

530 Acknowledgments

531 This work was carried out in part during the internship time of Kassoum YAMBA at the
532 International Data centre of the Comprehensive nuclear-Test-Ban-Treaty Organization
533 (SA/IDC/CTBTO).

534 Disclaimer

535 The views expressed by the authors in this work do not necessarily reflect those of the
536 CTBTO.

537 References

538

- 539 Axelsson, A., Ringbom, A., 2014. On the calculation of activity concentrations and nuclide
540 ratios from measurements of atmospheric radioactivity. *Appl. Radiat. Isot.* 92, 12–17.
541 <https://doi.org/10.1016/j.apradiso.2014.05.020>
- 542 Carrigan, C.R., Sun, Y., Simpson, M.D., 2019. The characteristic release of noble gases from
543 an underground nuclear explosion. *J. Environ. Radioact.* 196, 91–97.
544 <https://doi.org/10.1016/j.jenvrad.2018.10.015>
- 545 DE GEER L.-E., MARSHALL Peter, ROZGONOVA Daniela, WEISS Wolfgang, 2001.
546 Comprehensive nuclear-test-ban treaty : relevant radionuclides. *Kerntech.* 1987 66,
547 113–120.
- 548 Galan, M., 2017. RADIOXENONS NUCLEAR DATA EVALUATIONS PROJECT.
- 549 Galan, M., Kalinowski, M., Gheddou, A., Yamba, K., 2018. New evaluated radioxenon decay
550 data and its implications in nuclear explosion monitoring. *J. Environ. Radioact.*
551 <https://doi.org/10.1016/j.jenvrad.2018.02.015>
- 552 Gueibe, C., Kalinowski, M.B., Baré, J., Gheddou, A., Krysta, M., Kusmierczyk-Michulec, J.,
553 2017. Setting the baseline for estimated background observations at IMS systems of
554 four radioxenon isotopes in 2014. *J. Environ. Radioact.* 178–179, 297–314.
555 <https://doi.org/10.1016/j.jenvrad.2017.09.007>

556 INTERNATIONAL ATOMIC ENERGY AGENCY, 2015. The Fukushima Daiichi Accident Technical -
557 Technical Volume 1/5 Description and Context of the Accident. IAEA.

558 Kalinowski, M., Liao, Y.-Y., Pistner, C., 2014. Discrimination of Nuclear Explosions against
559 Civilian Sources Based on Atmospheric Radioiodine Isotopic Activity Ratios. *Pure*
560 *Appl. Geophys.* 171, 669–676. <https://doi.org/10.1007/s00024-012-0564-7>

561 Kalinowski, M.B., 2011. Characterisation of prompt and delayed atmospheric radioactivity
562 releases from underground nuclear tests at Nevada as a function of release time. *J.*
563 *Environ. Radioact.* 102, 824–836. <https://doi.org/10.1016/j.jenvrad.2011.05.006>

564 Kalinowski, M.B., Axelsson, A., Bean, M., Blanchard, X., Bowyer, T.W., Brachet, G., Hebel, S.,
565 McIntyre, J.I., Peters, J., Pistner, C., Raith, M., Ringbom, A., Saey, P.R.J., Schlosser, C.,
566 Stocki, T.J., Taffary, T., Kurt Ungar, R., 2010. Discrimination of Nuclear Explosions
567 against Civilian Sources Based on Atmospheric Xenon Isotopic Activity Ratios. *Pure*
568 *Appl. Geophys.* 167, 517–539. <https://doi.org/10.1007/s00024-009-0032-1>

569 Kalinowski, M.B., Pistner, C., 2006. Isotopic signature of atmospheric xenon released from
570 light water reactors. *J. Environ. Radioact.* 88, 215–235.
571 <https://doi.org/10.1016/j.jenvrad.2006.02.003>

572 Kalinowski, M.B., Tuma, M.P., 2009. Global radioxenon emission inventory based on nuclear
573 power reactor reports. *J. Environ. Radioact.* 100, 58–70.
574 <https://doi.org/10.1016/j.jenvrad.2008.10.015>

575 LNHB, C., 2017. Library for gamma and alpha emissions [WWW Document]. Nucléide - Lara.
576 URL <http://www.nucleide.org/Laraweb/> (accessed 5.1.17).

577 Nir-El, Y., 2006. Dating the age of a recent nuclear event by gamma-spectrometry. *J.*
578 *Radioanal. Nucl. Chem.* 267, 567–573. <https://doi.org/10.1007/s10967-006-0088-7>

579 Nir-El, Y., 2004. Dating the age of a nuclear event by gamma spectrometry. *Proc. 14th Int.*
580 *Conf. Radionucl. Metrol. Its Appl. ICRM 2003* 60, 197–201.
581 <https://doi.org/10.1016/j.apradiso.2003.11.016>

582 NNDC, 2017. Evaluated Nuclear Structure Data File [WWW Document]. *Natl. Nucl. Data*
583 *Cent. Databases - Eval. Nucl. Struct. Data File Search Retr.* URL
584 <http://www.nndc.bnl.gov/ensdf/> (accessed 5.1.17).

585 Postelt, F., 2014. Potential of Spectrum Categorisation Concepts using Radionuclide Ratios
586 for Comprehensive Nuclear-Test-Ban Treaty Verification. *Pure Appl. Geophys.* 171,
587 693–697. <https://doi.org/10.1007/s00024-012-0577-2>

588 Schoengold, C.R., DeMarre, M.E., Kirkwood, E.M., 1996. Radiological Effluents Released from
589 U.S. Continental Tests between 1961 through 1992 (No. NV-317 (Rev 1) UC-702). U.S.
590 Department of Energy Rep, USA.

591 Yamba, K., Kalinowski, B.M., Sanogo, O., 2018a. On the usability of event zero time
592 determinations using radioxenon isotopic activity ratios given the real atmospheric
593 background observations (IV). Presented at the Workshop on Signatures of Man-
594 Made Isotope Production (WOSMIP VII), ResearchGate, Sydney, Australia.
595 [https://doi.org/DOI: 10.13140/RG.2.2.27645.00480](https://doi.org/DOI:10.13140/RG.2.2.27645.00480)

596 Yamba, K., Kalinowski, B.M., Sanogo, O., 2017a. On the usability of event zero time
597 determinations using radioxenon isotopic activity ratios given the real atmospheric
598 background observations (II). Presented at the SCIENCE AND TECHNOLOGY
599 CONFERENCE (SnT2017), ResearchGate, Vienna, Austria. [https://doi.org/DOI:](https://doi.org/DOI:10.13140/RG.2.2.15062.09283)
600 [10.13140/RG.2.2.15062.09283](https://doi.org/DOI:10.13140/RG.2.2.15062.09283)

601 Yamba, K., Kalinowski, B.M., Sanogo, O., 2017b. On the usability of event zero time
602 determinations using radioxenon isotopic activity ratios given the real atmospheric

603 background observations (III). Presented at the International Noble Gaz experiement
604 (INGE2017), ResearchGate, Norway/Middlesex, United Kingdom of Great Britain and
605 Northern Ireland. <https://doi.org/DOI: 10.13140/RG.2.2.35194.75200/1>
606 Yamba, K., Kalinowski, B.M., Sanogo, O., 2016a. On the usability of event zero time
607 determinations using radioxenon isotopic activity ratios given the real atmospheric
608 background observations (I). Presented at the Workshop on Signatures of Man-Made
609 Isotope Production (WOSMIP VI), ResearchGate, Bariloche, Argentina.
610 <https://doi.org/DOI: 10.13140/RG.2.2.10028.92806>
611 Yamba, K., Kalinowski, B.M., Sanogo, O., Koulidiati, J., Nikkinen, M., 2015. Using radioxenon
612 concentrations for dating a nuclear event. Presented at the International Noble Gaz
613 experiement INGE2015, Austin, Texas, Usa. [https://doi.org/DOI:](https://doi.org/DOI: 10.13140/RG.2.2.11907.81441)
614 [10.13140/RG.2.2.11907.81441](https://doi.org/DOI: 10.13140/RG.2.2.11907.81441)
615 Yamba, K., Kalinowski, M.B., Sanogo, O., 2018b. Nuclear event zero time determination using
616 analytical solutions of radioxenon activities under in-growth condition. *Appl. Radiat.*
617 *Isot.* 139, 217–223. <https://doi.org/10.1016/j.apradiso.2018.04.020>
618 Yamba, K., Sanogo, O., Kalinowski, M.B., Nikkinen, M., Koulidiati, J., 2016b. Fast and accurate
619 dating of nuclear events using La-140/Ba-140 isotopic activity ratio. *Appl. Radiat. Isot.*
620 112, 141–146. <https://doi.org/10.1016/j.apradiso.2016.03.013>
621

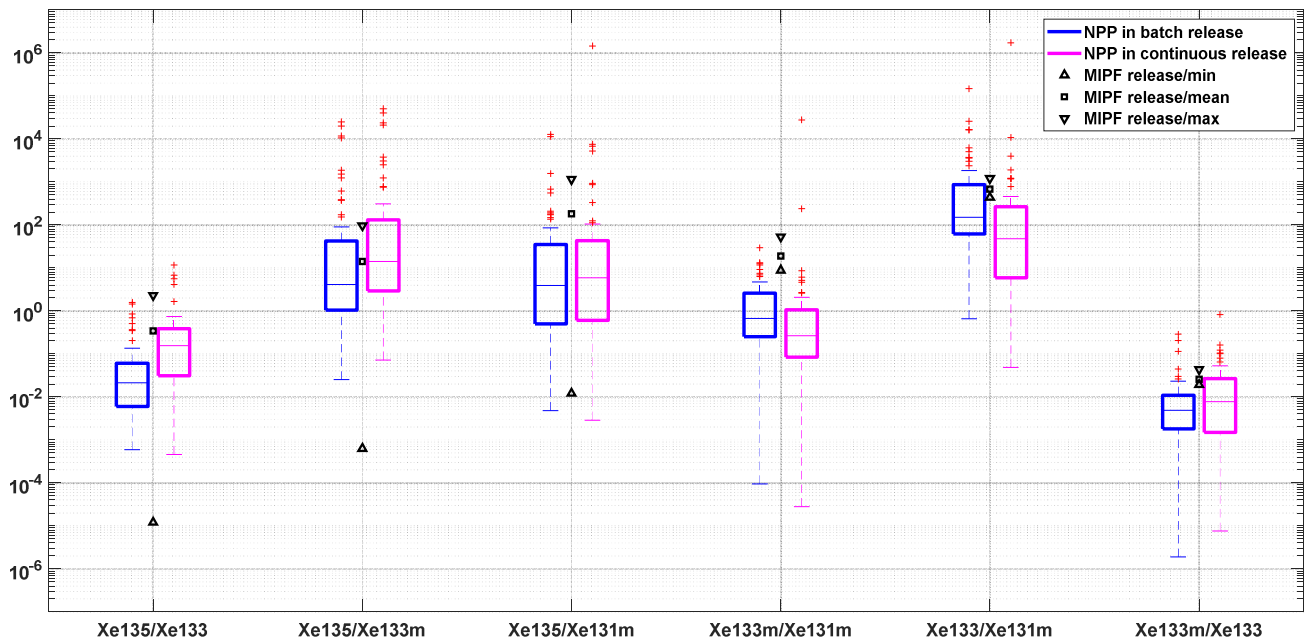


Figure 1: Distribution of radioxenon activity ratios using nuclear reactor (NPP) release data (Kalinowski and Tuma, 2009) and medical isotopes production facility (MIPF) release estimates (Kalinowski/Grosch/Hebel, 2014). Only batch release mode was considered for the nuclear event characterization in this study.

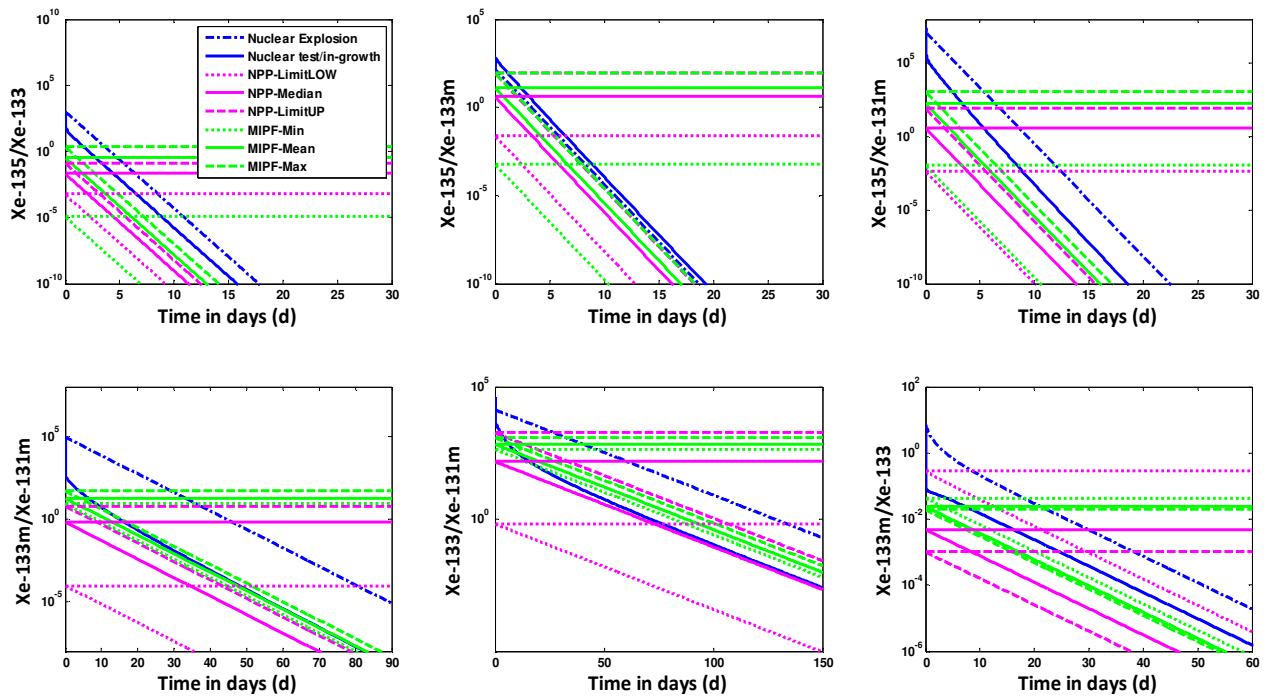


Figure 1: Change over time of isotopic activity ratios of CTBT-relevant radioxenons for two kinds of release from a nuclear explosion, and three indicative values of release from NPP and MIPF releases (minimum, median and maximum). The latter are shown as constants as well in order to account for the fact that such fresh pulse releases can occur at any time after the assumed time zero of a nuclear explosion scenario.

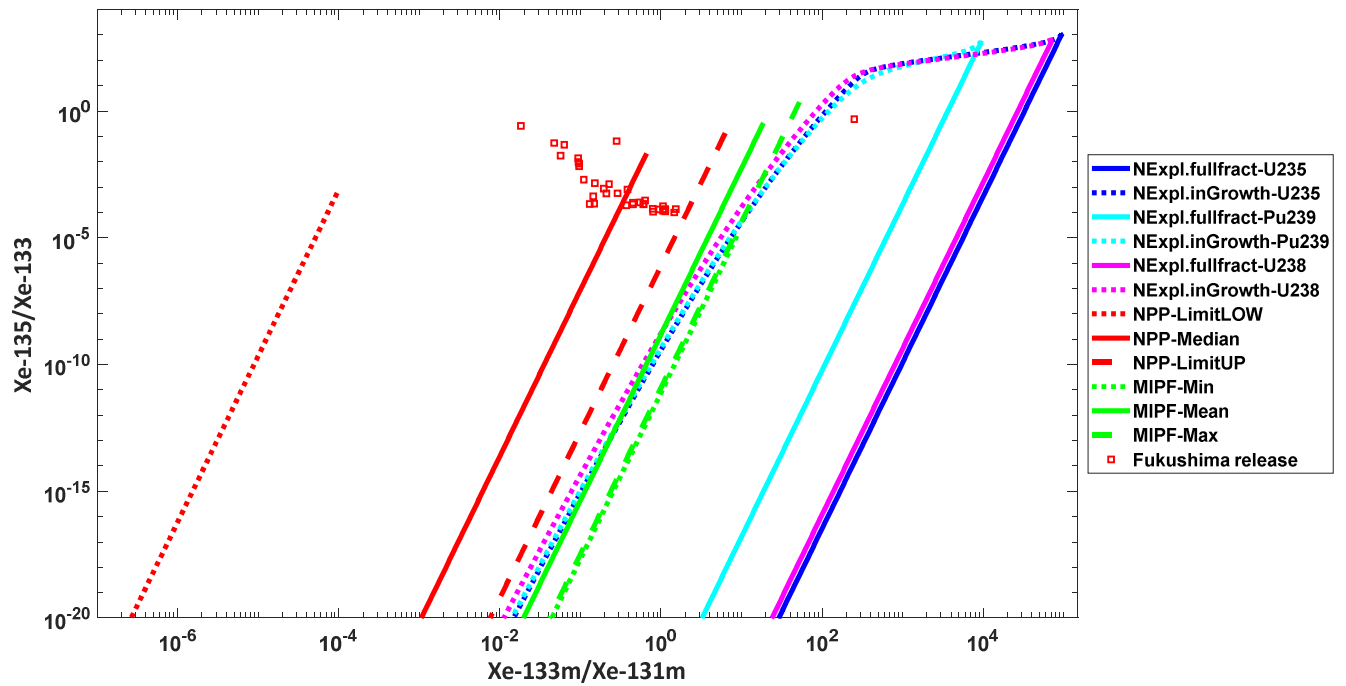


Figure 1: Change of radioxenon activities ratios $Xe135/Xe133$ against $Xe133m/Xe131m$ according to the kind of releases. The initial isotopic activity ratios (activity ratios at the release) used for nuclear reactor releases (NPP-median, NPP-limitLOW and NPP-limitUP) and medical isotopes production facilities releases (MIPF-mean, MIPF-min and MIPF-max) are respectively from Table1 and Table2. The square red dots represent debris released from Fukushima accident as observed at IMS stations.

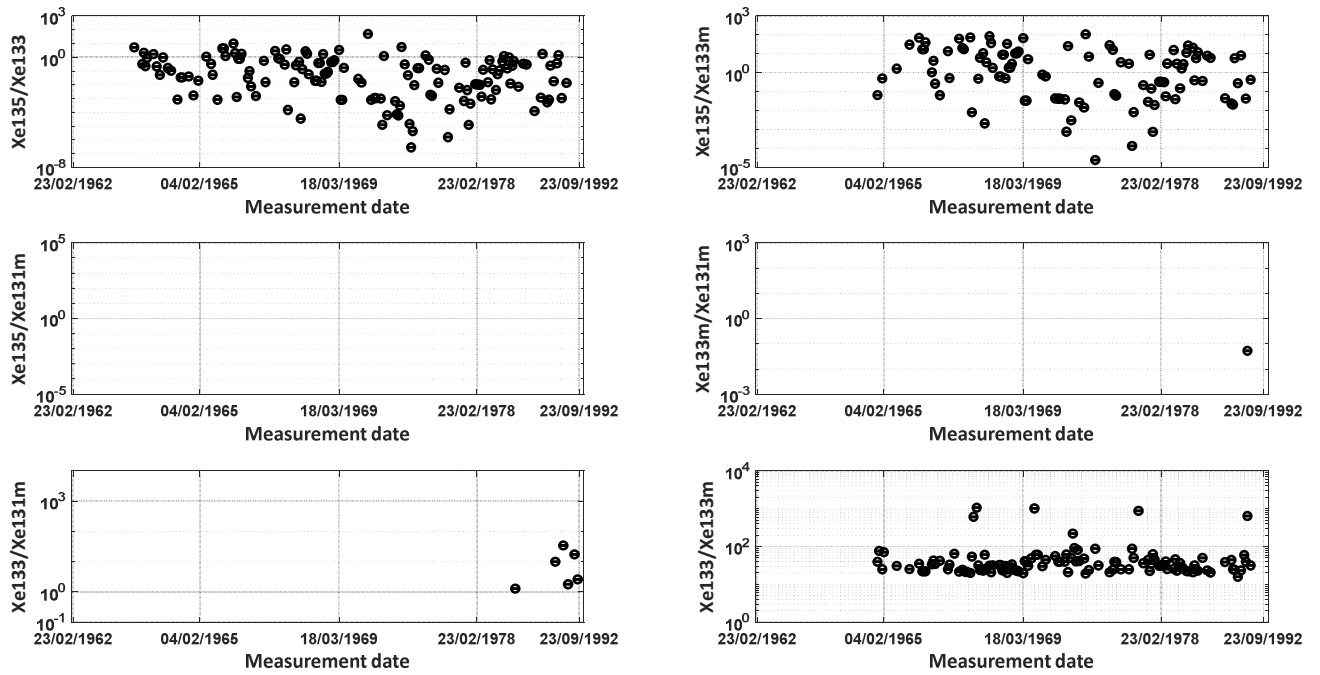


Figure 1: Distribution of the valid activity ratios using Nevada nuclear explosion data. We can notice that the ratios including Xe-131m, namely Xe-135/Xe-131m, Xe-133/Xe-131m and Xe-133m/Xe-131m are almost absent.

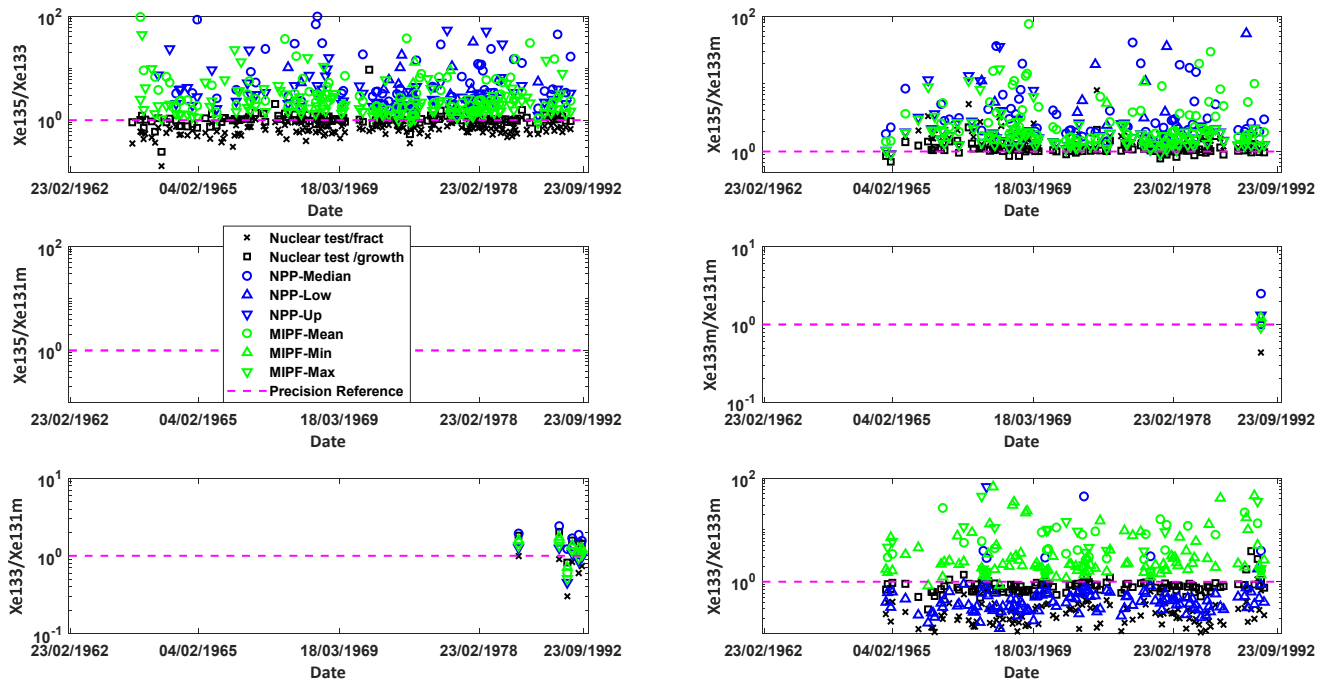


Figure 1: Distribution of the evaluated age precision according to the kind of release. Useful Nevada xenon activity ratios were used in the time algorithms for Nuclear explosions (full fractionation and under in-growth conditions), NPPs release (median, lower limit and upper limit values), MIPFs release (mean, min and and max values). The ideal age precision shown in magenta colour is normalized to 1.

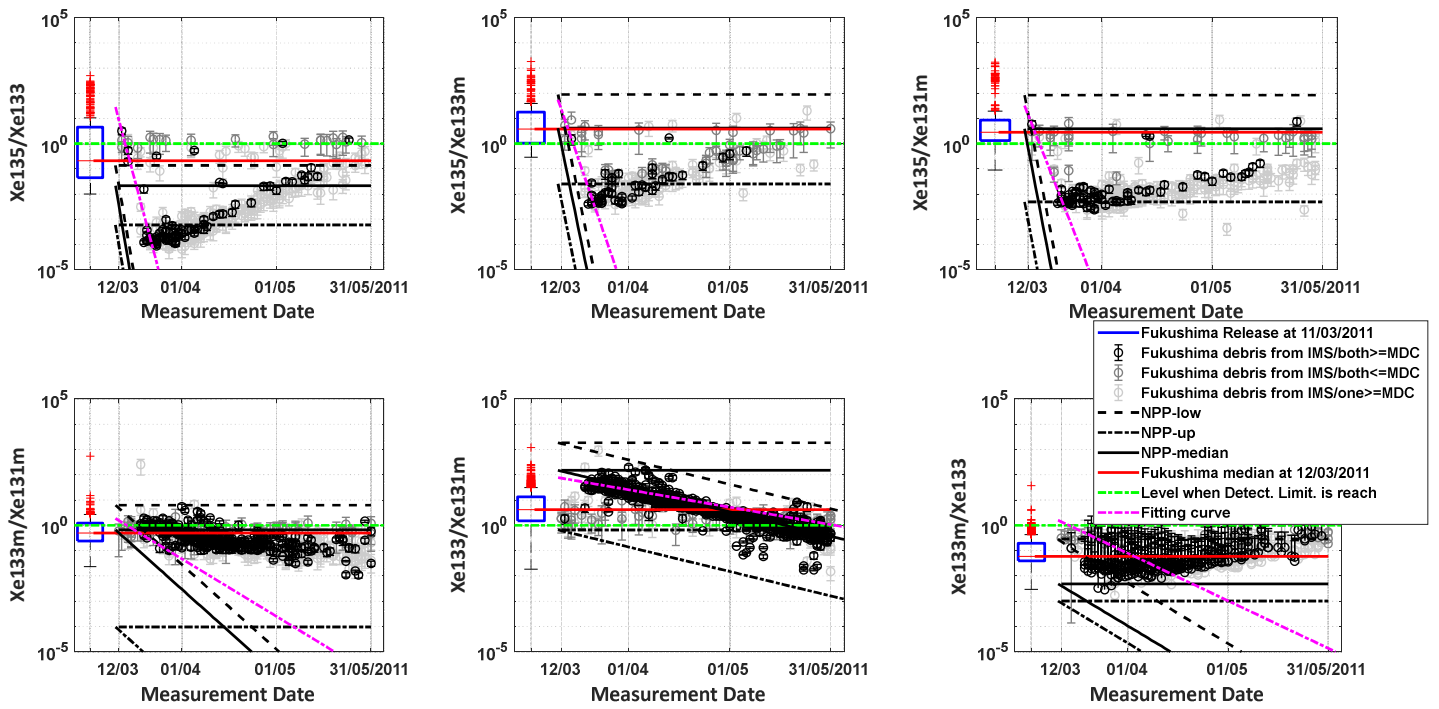


Figure 1: Distribution of the activity ratios using Fukushima accident debris data. Data used in this study were recorded from 14/03/2011 to 31/05/2011 in many IMS radionuclide stations. Black colour is used for valid entries for which both isotopes are above MDC, i.e. real detections that can be quantified; a bright grey is used in case one of the two isotopes is above MDC (in general it is the longer lived one of both); a dark grey indicates ratios that are calculated with both isotopes below MDC and basically scatter around the ratio of both isotopes detection limit, i.e. close to 0 in the logarithmic scale (indicated by a green line).

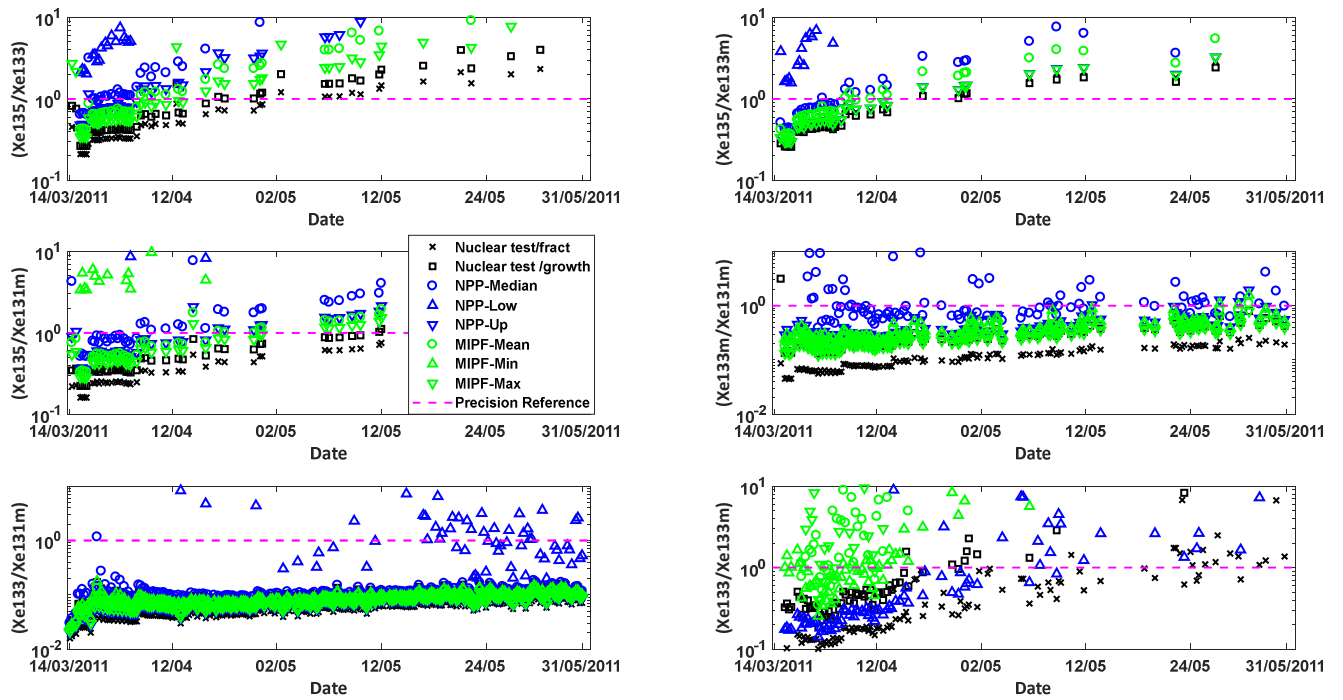


Figure 1: Distribution of the evaluated age precision according to the kind of release. Useful activity ratios from Fukushima accident debris were used in the time algorithms for Nuclear explosions (full fractionation and under in-growth conditions), NPPs release (median, lower limit and upper limit values), MIPFs release (mean, min and and max values). The ideal age precision shown in magenta colour is normalized to 1.

Table 1: Reported xenon activity ratios from nuclear reactors releases, measured by Nuclear Power Plants (NPP) in United States and Europe during 2006, 2009 and 2014. Only the batch release cases were considered.

Observations of data released from NPPs			
<i>Activity ratio</i>	<i>Lower Limit</i>	<i>Median</i>	<i>Upper Limit</i>
<i>Xe-135/Xe-133m</i>	2.5E-02	4.1E+00	9.0E+01
<i>Xe-135/Xe-133</i>	5.9E-04	2.1E-02	1.4E-01
<i>Xe-135/Xe-131m</i>	4.8E-03	3.9E+00	8.5E+01
<i>Xe-133m/Xe-133</i>	1.9E-06	4.9E-03	2.3E-02
<i>Xe-133m/Xe-131m</i>	9.6E-05	6.6E-01	6.3E+00
<i>Xe-133/Xe-131m</i>	6.6E-01	1.5E+02	1.8E+03

Table 1: Reported xenon activity ratios from medical isotopes production facility (MIPF) releases. Only the batch release cases were considered.

Observations of data released from MIPFs			
<i>Activity ratio</i>	<i>Lower Limit</i>	<i>Median</i>	<i>Upper Limit</i>
<i>Xe-135/Xe-133m</i>	6.9E-04	1.4E+01	9.6E+01
<i>Xe-135/Xe-133</i>	1.2E-05	3.4E-01	2.3E+00
<i>Xe-135/Xe-131m</i>	1.2E-02	1.8E+02	1.2E+03
<i>Xe-133m/Xe-133</i>	1.9E-02	2.6E-02	4.3E-02
<i>Xe-133m/Xe-131m</i>	8.8E+00	1.9E+01	5.3E+01
<i>Xe-133/Xe-131m</i>	4.4E+02	6.8E+02	1.2E+03

Table 1: Evaluation of the time precision difference obtained by making the difference between the perfect time precision value and the found time precision. The observation data used are from Nevada underground nuclear test. Plutonium Pu-239 and Uranium U-235 are used as the nuclear explosion materials fission induced by fission energy neutrons.

Statistical analysis (median) of the age precision difference							
Nuclear event		Xe135/Xe133	Xe135/Xe133m	Xe135/Xe131m	Xe133m/Xe131m	Xe133/Xe131m	Xe133/Xe133m
Pu-239	N. Expl. f.fract	0.2903	0.6082	NaN	0.4793	0.2280	0.7726
	N. Expl. growth	0.0751	0.1083	NaN	0.0118	0.5818	0.2959
U-235	N. Expl. f.fract	0.3481	0.3311	NaN	0.5627	0.2110	0.7724
	N. Expl. growth	0.0741	0.0789	NaN	0.0183	0.5188	0.2098
	NPP median	2.6589	1.5214	NaN	1.4976	0.7769	2.5316
	NPP lower	4.3000	4.7001	NaN	NaN	NaN	0.5963
	NPP upper	1.7944	0.5569	NaN	0.3197	0.1993	116.8618
	MIPF mean	1.3537	1.0305	NaN	0.0738	0.3275	3.3704
	MIPF min	7.9886	4.2179	NaN	0.2324	0.3255	1.1981
	MIPF max	0.8425	0.5268	NaN	0.0868	0.2485	3.6374

Activities data used are from US Nevada nuclear test site (Pu-239&U-235 material)

Table 1 : Evaluation of the time precision difference obtained by making the difference between the perfect time precision value and the found time precision. The observation data used are from Fukushima accident debris. Plutonium Pu-239 and Uranium U-235 are used as the nuclear explosion materials fission induced by fission energy neutrons.

Statistical analysis (median) of the age precision difference							
Nuclear event		Xe135/Xe133	Xe135/Xe133m	Xe135/Xe131m	Xe133m/Xe131m	Xe133/Xe131m	Xe133/Xe133m
Pu-239	N. Expl. f.fract	0.6354	0.4877	0.6141	0.8747	0.9292	0.7464
	N. Expl. growth	0.5798	0.5604	0.5376	0.7575	0.8973	0.7511
U-235	N. Expl. f.fract	0.6020	0.5231	0.6696	0.8955	0.9463	0.7462
	N. Expl. growth	0.5806	0.5625	0.5421	0.7592	0.9006	0.7439
	NPP median	0.3574	0.3397	0.4666	0.3402	0.8895	NaN
	NPP lower	3.9186	3.8733	24.7226	NaN	0.6575	0.7589
	NPP upper	0.4581	0.4908	0.4605	0.6316	0.9321	NaN
	MIPF mean	0.3718	0.3839	0.4765	0.7216	0.9205	1.4539
	MIPF min	NaN	NaN	4.7126	0.6635	0.9133	0.3816
	MIPF max	0.5196	0.4947	0.5385	0.7736	0.9281	0.8098

Activities data used are from Fukushima accident (Pu-239&U-235 material)

Table 1: Statistics obtained using a confusion matrix. Activities data used are from Nevada test. For each nuclear event, five (05) isotopic activity ratios are considered.

Nuclear Event	Statistic (5 items used)			
	TP	FP	TN	FN
N.E full fract	--	0	5	--
N.E growth	4	--	--	1
NPP	--	1	4	--
MIPF	--	0	5	--

Activities data used are from US Nevada nuclear test site

TP: True Positive, FP: False Positive, TN: True Negative, FN: False Negative

Table 1: Statistics obtained using a confusion matrix. Activities data used are from Fukushima accident. For each nuclear event, six (06) isotopic activity ratios are considered.

Nuclear Event	Statistic (6 items used)			
	TP	FP	TN	FN
N.E full fract	--	0	6	--
N.E growth	--	0	6	--
NPP	5	--	--	1
MIPF	--	1	5	--

Activities data used are from Fukushima accident

TP: True Positive, FP: False Positive, TN: True Negative, FN: False Negative